Building bridges between nuclear structure and reactions

Jutta E. Escher[1,*], *Emanuel V.* Chimanski[2], *Marc* Dupuis[3], *Eun Jin* In[1], *Sophie* Péru[3], *Aaina* Thapa[1], and *Walid* Younes[1]

[1]Lawrence Livermore National Laboratory, Livermore, California 94551, USA
[2]Brookhaven National Laboratory, Upton, NY 11973, USA
[3]CEA DAM DIF, F-91297, Arpajon, France *and* Université Paris-Saclay, CEA, LMCE, 91680 Bruyères-le-Châtel, France

Abstract. The past couple of decades have seen tremendous advances in nuclear structure and reaction theory. Innovative theory frameworks for describing the nuclear many-body system, increasingly powerful computers, and opportunities for confronting theory predictions with data on unstable nuclei, have been driving the field. An important goal is to move from phenomenological ingredients in reaction calculations to predictive theories based on microscopic frameworks. We discuss ongoing efforts aimed at integrating microscopic descriptions of nuclear structure into reaction predictions for medium-mass and heavy nuclei. This contribution highlights areas where Eric Bauge, a champion for building bridges, has made important contributions by encouraging and enabling collaborations between communities with complementary expertise.

1 Introduction

With the advent of radioactive beams we can now tackle questions about static and dynamic properties of not only stable, but also exotic nuclei. This gives us opportunities to test theory predictions and to plan experiments that uncover systematic trends in nuclei, such as the evolution of shell structure, nuclear deformation, and collective modes of excitation. We need improved reaction theory to develop signatures that experiments can look for and to interpret the findings [1]. We also want to calculate structure and reaction inputs for applications: Astrophysics simulations, for instance, require nuclear structure and reaction information for unstable nuclei. Many of these nuclei will be accessible experimentally, but only a small portion will be measured [2, 3], thus measurements need to be complemented by theoretical predictions.

To make progress on both these fronts, we need to integrate nuclear structure and reaction theory. In the last decade or so there has been significant progress in moving towards much more sophisticated and predictive descriptions of reactions involving light nuclei [4]. This was a logical extension of the *ab initio* nuclear structure descriptions that were developed in the early 2000s and that continue to be extended [5]. The resonating group method (RGM) is a useful approach for combining structure and reactions. For binary reactions, it starts with an expansion of the full wave function into cluster wave functions that incorporate the *ab initio* structure information. One then solves the Hill-Wheeler equations to obtain the relative wave function which in turn can be used to calculate reaction observables. Applications of the RGM with the no-core shell model (NCSM) as its structure component have been very successful for light nuclei [6]. A major advantage is that the approach treats structure and reactions on the same footing and utilizes state-of-the-art nuclear interactions including 2-body and 3-body forces. The NCSM/RGM approach can also be cast in a framework that uses a symmetry-adapted basis [7]. The extra complication that arises from using a more complicated [SU(3)] coupling scheme instead of the familiar angular-momentum coupling is offset by computational gains and the prospect of reaching heavier nuclei well beyond the p and sd shells [8, 9].

Most descriptions of reactions with medium-mass and heavy nuclei ($A \geq 20$) do not use the RGM approach, but make significant simplifications. Normally, they treat direct and compound-nuclear reactions separately. For direct reactions, one often starts with a simplified picture in which the internal structure of the interacting nuclei is ignored and focuses on the reaction mechanism. Cross sections are typically normalized to reproduce data. This clearly limits the predictive power of such calculations. Given the availability of sophisticated structure models for medium-mass and heavy nuclei, it is worthwhile to develop reaction descriptions that utilize their structure predictions. Here we discuss an approach that integrates structure information from Hartree-Fock Bogoliubov (HFB) theory and the Quasiparticle Random-Phase Approximation (QRPA) into a coupled-channels reaction framework.

2 Integrated theory for direct scattering

Our focus is on developing structure and reaction tools that can be applied to a large number of isotopes, including heavy deformed nuclei. We use HFB+QRPA structure theory, based on the Gogny finite-range interaction and implemented in an axially-symmetric deformed ba-

*e-mail: escher1@llnl.gov

sis [10, 11]. This structure approach has been successfully employed to describe properties of nuclear ground states, as well as excitations at low and high energies [12]. It is particularly well suited to provide structure input for coupled-channels calculations of elastic and inelastic scattering [13–16]. The expected outcome will be a computational capability that predicts neutron scattering observables for nuclear data evaluations [17–19], charged-particle scattering for surrogate reaction applications [20–24], and that enables the study of fundamental nuclear properties both near and away from the valley of stability [25].

We start from a set of coupled-channels equations for binary reactions:

$$\left\{\frac{d^2}{dr^2}-\frac{l_c(l_c+1)}{r^2}-\frac{2\mu_c}{\hbar^2}V^J_{cc}(r)+k_c^2\right\}u_c(r) = \sum_{c'\neq c}\frac{2\mu_{c'}}{\hbar^2}V^J_{cc'}(r)u_{c'}(r)\ , \quad (1)$$

where $u_c(r)$ is the relative-motion wave function in channel c, r the distance between projectile and target, μ_c the reduced mass, l_c denotes the relative angular momentum, and k_c the relative momentum; $V^J_{cc'}$ is the potential that couples the ground states of target and projectile to the relevant excited states, and the diagonal term V^J_{cc} is the optical potential for channel c. At present, we consider only elastic and inelastic scattering, *i.e.* we have the same projectile and target nuclei in the initial and final channels.

For inelastic nucleon-nucleus scattering, $V^J_{cc'}$ involves a sum over angular-momentum recoupling coefficents and folding integrals of the form

$$4\pi\sqrt{2I_c+1}\int_0^\infty dr_t r_t^2 v_L^{ST}(r,r_t)\rho^{Tq,cc'}_{LSJ}(r_t)\ , \quad (2)$$

where I_c denotes the target spin, $v_L^{ST}(r,r_t)$ is the effective interaction between the projectile nucleon at r and a target nucleon at r_t, and $\rho^{Tq,cc'}_{LSJ}(r_t)$ is the (radial) transition density that is obtained from the QRPA structure calculation for the target nucleus. Here L,S,J,T denote the change in orbital angular momentum, spin, total angular momentum, and isospin of the target nucleus. We use the JLMB variant of the Jeukenne-Leujene-Mahaux (JLM) effective nucleon-nucleon interaction, developed by Bauge *et al.* [26–29]. For cases with a composite projectile that can be excited an analogous projectile folding term enters the coupling potentials.

The structure information obtained from HFB+QRPA calculations is encoded in the ground state and transition densities; the folding procedure and subsequent use of the coupling potentials in a coupled-channels or distorted-wave Born approximation (DWBA) calculation effectively integrates structure and scattering calculations. The advantage of this integrated microscopic approach over calculations with phenomenological coupling potentials is that it allows for scattering predictions when there is no data to scale the cross sections.

3 Results for selected nuclei

The applications we are interested in involve elastic scattering and inelastic scattering to both low-lying states (up to $E_{ex}\approx 3$ MeV) and higher-energy states (up to $E_{ex}\approx 30$ MeV). Consequently, the structure model chosen must be able to provide reliable information on such states. We employ the D1M parametrization of the finite-range Gogny force, which was introduced to provide reliable properties for both nuclear matter and finite nuclei, including masses, radii, giant resonances, and fission [12].

3.1 Ground states of Zr isotopes

Within our HFB framework, which uses an axially-symmetric deformed basis and includes the complete Coulomb interaction also in the pairing fields, we obtain ground state properties that are in good agreement with alternative predictions and experimental data. In Fig. 1 we show predicted ground state deformation, binding energy per nucleon (BE/A), and relative charge radius shifts (δr_c^2, relative to the value for ^{90}Zr) for the chain of even-even zirconium isotopes, from A=78 to A=122. Experimental binding energies are well reproduced. The charge radius shifts and deformations are mostly in good agreement with experimental data, with deviations existing in cases where shape coexistence introduces additional correlations that are beyond the present work, but can be treated, e.g. with the Generator Coordinate Method (GCM). For a more detailed discussion, see Ref. [30].

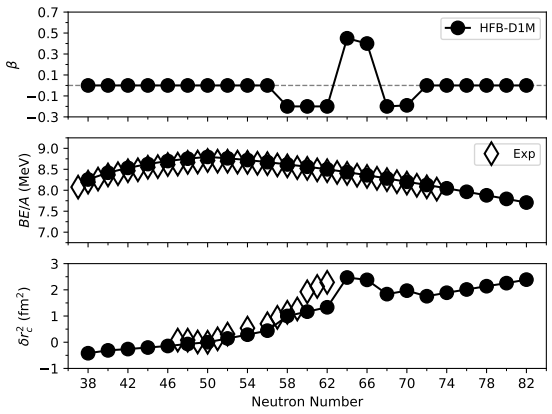

Figure 1. HFB predictions for ground state properties of the $^{78-122}Zr$ isotopes. Shown are β deformation (top panel), binding energy per nucleon BE/A (middle), and charge radius shift relative to ^{90}Zr (bottom). Where available, experimental data are shown for comparison.

3.2 States at low and high excitation energies in Zr

To obtain structure information for excited states, we build QRPA excitations on top of the calculated HFB minima, using the same basis and interaction to achieve a consistent overall treatment. Predicted energies for low-lying states, reduced electromagnetic strengths, specifically B(E2) and

B(E3) values, are found to be in reasonable agreement with experiment, see Ref. [30].

An attractive feature of the QRPA approach is that it can also describe collective excitations at tens of MeV. We have calculated monopole, dipole, quadrupole, and octupole responses for spherical and deformed Zr nuclei and found good agreement with available data or known systematics, see Ref.[30].

3.3 Microscopic structure of resonances in ^{92}Mo

Our QRPA approach provides us with a useful tool to investigate collective nuclear excitations, including the well-studied giant-dipole resonance (GDR) and the more exotic pygmy and toroidal dipole resonances [25, 31, 32]. Understanding the emergence of both single-particle and collective properties is, in general, an important goal of nuclear structure physics. Dipole resonances are of particular interest, as they are known to impact neutron capture reactions which are important for nuclear astrophysics simulations [33]. Understanding the mechanisms responsible for the occurrence of dipole resonances, their underlying structural properties, and their evolution with mass number, neutron excess, and deformation, will improve calculations of neutron-capture cross sections.

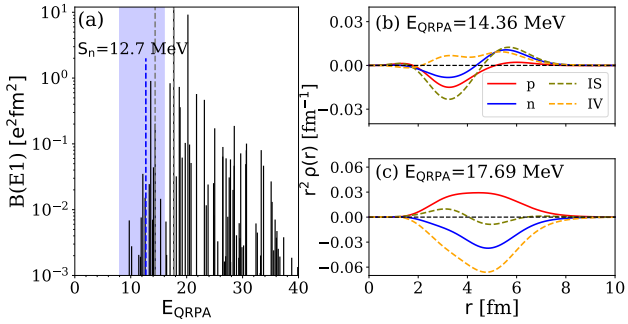

Figure 2. $J^\pi = 1^-$ excitation spectrum for ^{92}Mo (panel a) and transition densities for selected states. The state at $E_{ex} = 14.36$ MeV (panel b) exhibits neutron skin oscillations at the nuclear surface and both proton and neutron oscillations in the interior, while the state at 17.69 MeV (panel c) shows a pattern characteristic of an isovector giant-dipole oscillation.

QRPA calculations provide information on the energies of excited states and on the nature of the excitation. Transition densities (TDs) play an important role in the analysis of the structure of the excited states, as the TDs represent, for each state, changes relative to the ground state. An example is shown in Fig. 2 for ^{92}Mo. Panel (a) shows the B(E1) spectrum for this spherical nucleus. Panels (b) and (c) show the TDs for two excited states, selected from a region around the neutron separation energy ($S_n = 12.7$ MeV), indicated by the blue band.

The radial TDs are shown for states at $E_{ex} = 14.36$ MeV (panel b) and $E_{ex} = 17.69$ MeV (panel c). The TDs are given for neutrons and protons (solid blue and red curves) and also as isoscalar and isovector quantities (dashed black and orange curves), for easier interpretation. The two states exhibit clearly distinct behaviors. The pattern in panel (c) is characteristic of an isovector giant dipole state, while panel (b) shows strong neutron oscillation in the nuclear surface, behavior that is often associated with a pygmy dipole resonance (PDR).

This example illustrates that the region near S_n contains both PDR- and GDR-type excitations. This has implications for the interpretation of experiments that find an enhancement in the dipole response near S_n. More work is needed to disentangle the structure effects in a systematic manner.

3.4 Elastic and inelastic scattering predictions

To obtain predictions for elastic and inelastic scattering, we use the folding approach described above and in Refs. [15, 16] to produce coupling potentials $V^J_{cc}(r)$ and $V^J_{cc'}(r)$ for use in DWBA calculations with the coupled-channels code Fresco[34]. Results for proton scattering off ^{94}Zr at multiple incident proton energies are shown in Fig. 3. The results in panel (a) show excellent agreement with experimental data for $E_{beam} = 12.7$ MeV and 22.5 MeV. Panel (b) shows predictions for inelastic scattering to the first excited 3^- state in ^{94}Zr, for three different beam energies. Where data is available, the agreement is quite good. Similar results have been obtained for both proton and neutron scattering from other Zr isotopes [16].

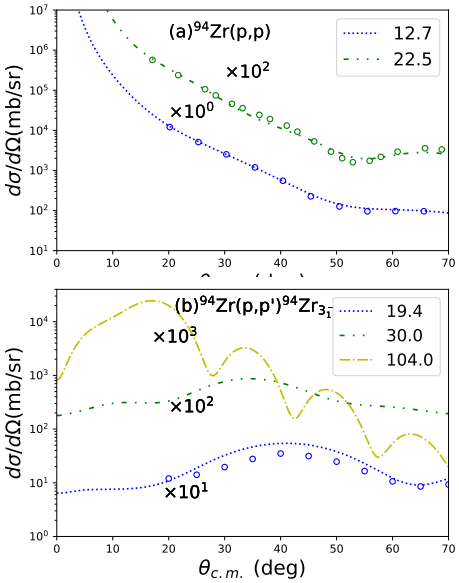

Figure 3. Predictions for elastic (top) and inelastic (bottom) proton scattering off ^{94}Zr, for various beam energies. The open circles represent experimental data [35–37]. The DWBA scattering calculations used the folded coupling potentials described in the text; they have not been fitted to the data, but are predictions. Curves and data have been scaled for better visibility.

Inelastic scattering to low-lying excitations in both spherical and deformed nuclei, including actinides, is important for improving nuclear data evaluations. Charged-particle inelastic scattering to higher-energy states is

needed to enable surrogate-reaction applications, which require calculated spin-parity populations for the surrogate reaction used. Charged-particle scattering can also be used to probe the resonance structure near the neutron separation energy. Extensions of the present integrated structure-and-reaction framework are being developed to address these challenges.

4 Concluding thoughts

Recent theoretical developments have made it possible to achieve very good predictions of nuclear structure properties for a large number of nuclei across the isotopic chart. The method described here integrates state-of-the-art HFB+QRPA nuclear structure calculations with a modern reaction approach to achieve a predictive capability for elastic and inelastic (direct) scattering. Developments are also needed to improve predictions of (direct) transfer reactions [38]. Furthermore, efforts are underway to integrate nuclear structure properties, such as level densities and γ-ray strength functions into the statistical descriptions of compound nuclear reactions [39].

Building bridges between nuclear structure and reactions is critical for achieving predictive reaction capabilities for both direct and compound nuclear reactions. Collaborations have played, and continue to play, an important role in advancing the relevant theoretical capabilities, in developing and validating codes, and for gaining physics insights. We remember Eric Bauge for his technical contributions to this field, and for enabling collaborations and building bridges between different communities.

This work was performed under the auspices of the U.S. Department of Energy by Lawrence Livermore National Laboratory under Contract DE-AC52-07NA27344, with support from LDRD projects 19-ERD-017, 24-ERD-023.

References

[1] B.A. Brown et al., Motivations for early high-profile FRIB experiments, arxiv.org/abs/2410.06144
[2] A. Arcones et al., Prog. Part. Nucl. Phys. **94**, 1 (2017). 10.1016/j.ppnp.2016.12.003
[3] H. Schatz et al., Journal of Physics G **49**, 110502 (2022). 10.1088/1361-6471/ac8890
[4] P. Navrátil et al., Physica Scripta **91**, 053002 (2016).
[5] H. Hergert, Front. Phys. **8**, 379 (2020).
[6] S. Quaglioni et al., Nuclear Physics News **30**, 12 (2020). 10.1080/10619127.2020.1752089
[7] K.D. Launey et al., Prog. Part. Nucl. Phys. **89**, 101 (2016). 10.1016/j.ppnp.2016.02.001
[8] K.D. Launey et al., Annual Review of Nuclear and Particle Science **71**, 253 (2021). 10.1146/annurev-nucl-102419-033316
[9] A. Mercenne et al., Comp. Phys. Commun. **280**, 108476 (2022). 10.1016/j.cpc.2022.108476
[10] S. Péru et al., Eur. Phys. J. A **50**, 88 (2014). 10.1140/epja/i2014-14088-7
[11] W. Younes et al., *A Microscopic Theory of Fission Dynamics* (Springer, Cham, 2019)
[12] L.M. Robledo et al., Journal of Physics G **46**, 013001 (2018). 10.1088/1361-6471/aadebd
[13] G.P.A. Nobre et al., Phys. Rev. Lett. **105**, 202502 (2010). 10.1103/PhysRevLett.105.202502
[14] G.P.A. Nobre et al., Phys. Rev. C **84**, 064609 (2011). 10.1103/PhysRevC.84.064609
[15] M. Dupuis et al., Phys. Rev. C **100**, 044607 (2019). 10.1103/PhysRevC.100.044607
[16] A. Thapa et al., EPJ Web Conf. **292**, 06003 (2024). 10.1051/epjconf/202429206003
[17] D. Brown et al., Nuclear Data Sheets **148**, 1 (2018). 10.1016/j.nds.2018.02.001
[18] M. Kerveno et al., Phys. Rev. C **104**, 044605 (2021). 10.1103/PhysRevC.104.044605
[19] J. Escher et al., EPJ Web of Conf. **284**, 03012 (2023). 10.1051/epjconf/202328403012
[20] J.E. Escher et al., Rev. Mod. Phys. **84**, 353 (2012). 10.1103/RevModPhys.84.353
[21] J.E. Escher et al., EPJ Web of Conferences **122**, 12001 (2016). 10.1051/epjconf/201612212001
[22] J.E. Escher et al., Phys. Rev. Lett. **121**, 052501 (2018). 10.1103/PhysRevLett.121.052501
[23] A. Ratkiewicz et al., Phys. Rev. Lett. **122**, 052502 (2019). 10.1103/PhysRevLett.122.052502
[24] R. Pérez Sánchez et al., Phys. Rev. Lett. **125**, 122502 (2020). 10.1103/PhysRevLett.125.122502
[25] E.J. In et al., (This volume, 04003)
[26] E. Bauge et al., Phys. Rev. C **61**, 034306 (2000). 10.1103/PhysRevC.61.034306
[27] E. Bauge et al., Phys. Rev. C **61**, 059902 (2000). 10.1103/PhysRevC.61.059902
[28] E. Bauge et al., Phys. Rev. C **63**, 024607 (2001). 10.1103/PhysRevC.63.024607
[29] E. Bauge et al., Phys. Rev. C **58**, 1118 (1998). 10.1103/PhysRevC.58.1118
[30] E.V. Chimanski et al., Coupling between collective modes in the deformed ^{98}Zr nucleus, arxiv.org/abs/2308.13374
[31] A. Bracco et al., Prog. Part. Nucl. Phys. **106**, 360 (2019). 10.1016/j.ppnp.2019.02.001
[32] E. Lanza et al., Prog. Part. Nucl. Phys. **129**, 104006 (2023). 10.1016/j.ppnp.2022.104006
[33] A. Tonchev et al., Physics Letters B **773**, 20 (2017). 10.1016/j.physletb.2017.07.062
[34] I.J. Thompson, Computer Phys. Rep. **7**, 167 (1988).
[35] J.B. Ball et al., Phys. Rev. **135**, B706 (1964). 10.1103/PhysRev.135.B706
[36] M.M. Stautberg et al., Phys. Rev. **151**, 969 (1966). 10.1103/PhysRev.151.969
[37] J.K. Dickens et al., Phys. Rev. **168**, 1355 (1968). 10.1103/PhysRev.168.1355
[38] C.W. Johnson et al., J. Phys. G **47**, 123001 (2020). 10.1088/1361-6471/abb129
[39] S. Hilaire et al., Towards More Predictive Nuclear Reaction Modelling, in *Compound-Nuclear Reactions*, ed. J.E. Escher et al. (Springer, 2021).